FACTOR ANALYSIS APPLIED TO GRAVITY PROFILES OF LUNAR IMPACT CRATERS. Carol B. Hundal[1], Alex J. Evans[1], John F. Mustard[1]. [1]Department of Earth, Environmental and Planetary Sciences, Brown University, Providence, RI, 02912. (carol_hundal@brown.edu).

Introduction: The crustal porosity structure of terrestrial worlds is substantially influenced by impact events [1]. Impacts can increase porosity by fracturing rock, dilatant bulking, and ballistic redistribution of materials. Alternatively, if the pre-impact crust is sufficiently porous, impacts can decrease this porosity through shockwave compaction, pore closure from localized heating, and induced magmatism.

The relationship between impact craters and porosity has been explored in many recent studies at the Moon using data from the Gravity Recovery and Interior Laboratory (GRAIL) mission [2; e.g., 3-6]. The Bouguer anomaly can be used to infer relative changes in porosity. An increase in porosity is broadly linked to decreased density and thus a decreased Bouguer anomaly. A significant impediment in quantifying impact-generated porosity is the isolation of the crater's induced gravitational signal from its surrounding region.

Here, we attempt to improve the isolation of a crater's gravity signal by: (1) reducing the gravity data to zonal harmonics centered on the crater's location and (2) applying factor analysis to groups of radial gravity profiles.

Background: Zonal harmonics are oriented like ripples about a center point, and they describe only radially oriented data. To a significant extent, craters are radially symmetric, and we hypothesize that removing azimuthal data will allow better isolation of gravitational signals correlated to the crater.

Factor analysis is a statistical technique that identifies independent axes of variance linked to latent variables. Eigenvectors produced by factor analysis show the dominant shapes of variance in the data when plotted against the original x variable. The first eigenvector describes the most variance with subsequent eigenvectors describing less variance.

We anticipate that factor analysis applied to gravity profiles will yield insights into the effects of impacts in GRAIL data. For example, factor analysis applied to gravity profiles may produce eigenvectors correlated to distinct impact-processes that influence porosity (e.g., fracturing, dilatant bulking, pore-closure due to heating, etc.).

Data: We use the GRGM1200bRM1 $\lambda = 1$ Bouguer anomaly gravity field calculated by [7] for degrees 7-600 with a crustal density of 2500 kg/m^3. This corresponds to a half-wavelength resolution of ~9 km.

The preliminary analyses are for 37 highland craters with diameter D of 60±5 km located between 0–60 ºN and 120–180 ºW [8]. Our preliminary analyses use a narrow diameter range in a localized region to minimize any size-dependent and compositional variations in crater gravity profiles.

Methods: First, we rotate the crater center to the north pole and reduce the gravity map of each crater to zonal harmonics of Bouguer anomaly data (Fig 2). A radial profile is constructed from the crater center out to three crater diameters. This profile is stored in terms of diameter-normalized distance.

For factor analysis, the data need to be pre-processed to a common sampling resolution and standardized to minimize regional variations. We (a) interpolate the profile to 50 points (similar to the resolution of the data), (b) subtract the profile by its mean, and (c) subsequently divide by the standard deviation. These pre-processed profiles are shown in Fig 3. All 37 profiles are processed in Python using Scikit-learn's factor analysis algorithm [9].

Preliminary Results: The gravity profiles of the highland craters broadly exhibit two main

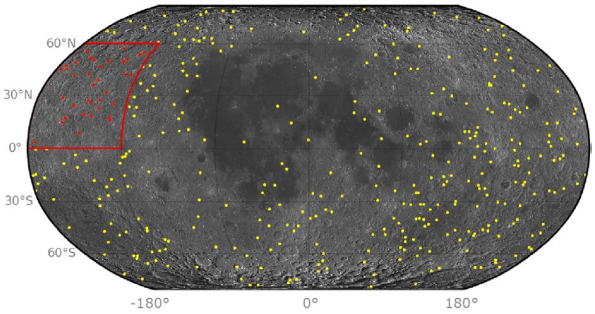

Fig 1. The 37 craters of this study are bounded by the red line between 0-60º N and 120-180ºW. Yellow dots show global distribution of craters D = 60±5 km.

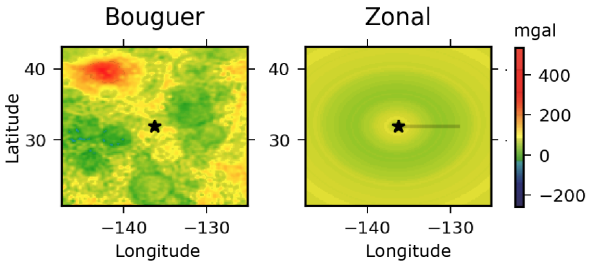

Fig 2. Converting Bouguer gravity anomaly data to zonal harmonics centered on the location of crater 02-1-001059 [8]. The grey line on the zonal map shows where the radial gravity profile was taken.

characteristics: a gravitational minimum within the crater interior and a gravitational maximum at the crater rim (Fig 3).

These trends are replicated in many, but not all, of the gravity profile eigenvectors produced by factor analysis (Fig 4). Eigenvector one exhibits a minimum inside the crater with an upward trend after the crater rim. Eigenvectors one through seven also show strong minima beneath the crater interior inside the crater rim. Eigenvector two also shows a negative signal where the continuous ejecta blanket is expected to occur. Eigenvectors two through seven show strong positive signals where the crater rim is expected.

We hypothesize the gravity minimum in the crater interior arises from increased porosity due to fracturing and dilatant bulking beneath the crater floor. The gravity maximum at the rim may be due to the elevation of the rim being closer to the GRAIL spacecraft, thus producing a stronger gravity signal. Eigenvectors two's diminished signal between 1-2D may be due to ballistic redistribution of material. This would have implications for using the ejecta area as a background region for the purposes of isolating a crater's induced gravitational signal from regional variations [e.g., 3].

Next Steps: Future analyses will compare the eigenvectors of craters of differing diameter ranges (e.g., 30±5 km, 90±5 km), states of preservation, and geochemical terranes. We will also employ methods similar to [3] to remove atypical gravity profiles to improve the interpretability of our results. This would include, for example, removing profiles where the the elevation of the crater interior is higher than its surroundings. Finally, dot-product mapping can be used to highlight regions where certain eigenvectors are more strongly expressed. This would help determine whether certain eigenvector shapes are correlated with distinct impact-crater processes.

Acknowledgements: Thanks to Kierra Wilk, Janie Levin, Matt Jones, and Fiona Nichols-Fleming for debugging help.

References: [1] Melosh, H. (1989) *Oxford University Press*. [2] Zuber M. T. et al. (2013) *Science* 339(6120) : 668-671. [3] Soderblom et al. (2015) *GRL* 42(17) , 6939-6944. [4] Wahl et al. (2020) *JGR : Planets* 125(4). [5] Venkatadri T. K. & James P. B. (2020) *Icarus* 352, 113953. [6] Bierson C. J. et al. *JGR* 121(8) `488-1497. [7] Goossens S. et al. (2020) *JGR Planets,* 125(2). [8] Robbins S. J. (2018) *JGR Planets, 124,* 871-892. [9] Pedregosa et al. (2011), *JMLR* 12, 2825-2830.

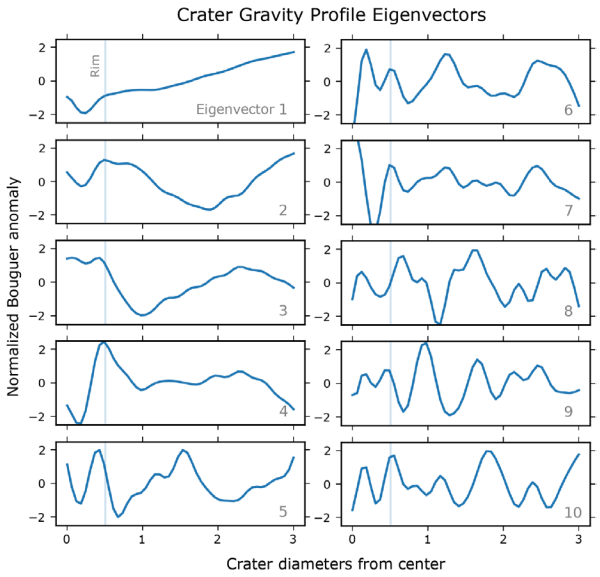

Fig 4. The first ten eigenvectors of the radial gravity profiles of the 37 craters indicated in Fig 1. The faint blue vertical line indicates the crater rim. Note that calculated eigenvectors are sign-agnostic and can be 'upside down'.

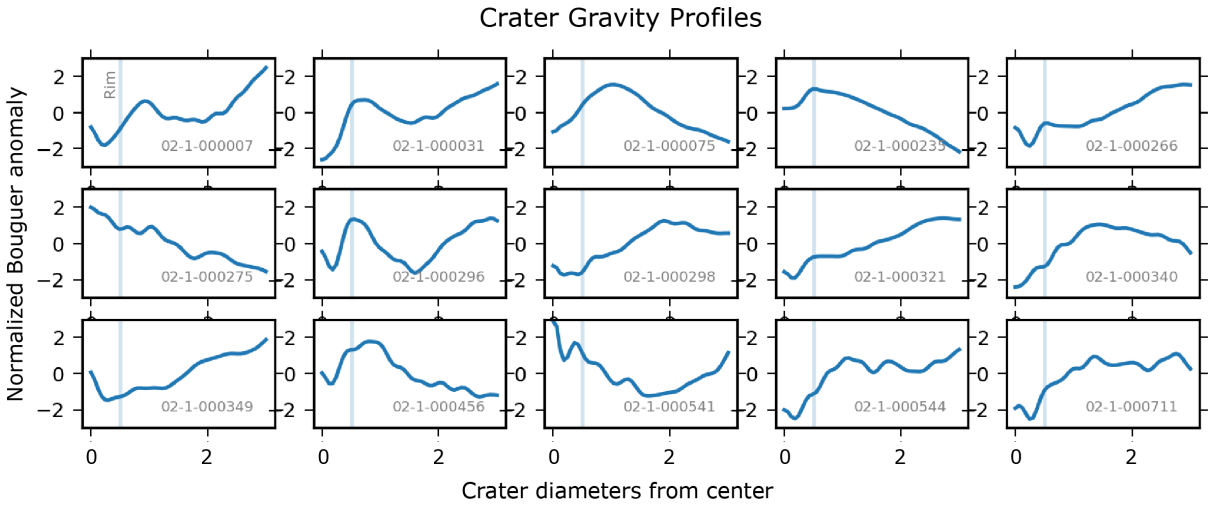

Fig 3. Normalized zonal gravitational profiles from 15 of the 37 craters shown in the red region of Figure 1. Profiles are taken from the crater center out to three crater diameters. The light blue line indicates the crater rim. Crater IDs from the Robbins et al. 2018 catalog [8] are indicated.